ACS Partner Journal
PRECISION CHEMISTRY
pubs.acs.org/PrecisionChem
Article

Synthesis of RNA-Amphiphiles via Atom Transfer Radical Polymerization in the Organic Phase

Jaepil Jeong, Grzegorz Szczepaniak, Subha R. Das,* and Krzysztof Matyjaszewski*

Cite This: *Precis. Chem.* 2023, 1, 326−331

Read Online

ACCESS | Metrics & More | Article Recommendations | Supporting Information

ABSTRACT: The combination of hydrophobic polymers with nucleic acids is a fascinating way to engineer the self-assembly behavior of nucleic acids into diverse nanostructures such as micelles, vesicles, nanosheets, and worms. Here we developed a robust route to synthesize a RNA macroinitiator with protecting groups on the 2′-hydroxyl groups in the solid phase using an oligonucleotide synthesizer. The protecting groups successfully solubilized the RNA macroinitiator, enabling atom transfer radical polymerization (ATRP) of hydrophobic monomers. As a result, the RNA−polymer hybrids obtained by ATRP exhibited enhanced chemical stability by suppressing cleavage. In addition, we demonstrated evidence of controlled polymerization behavior as well as control over the molecular weight of the hydrophobic polymers grown from RNA. We envision that this methodology will expand the field of RNA−polymer conjugates while vastly enhancing the possibility to alter and engineer the properties of RNA-based polymeric materials.

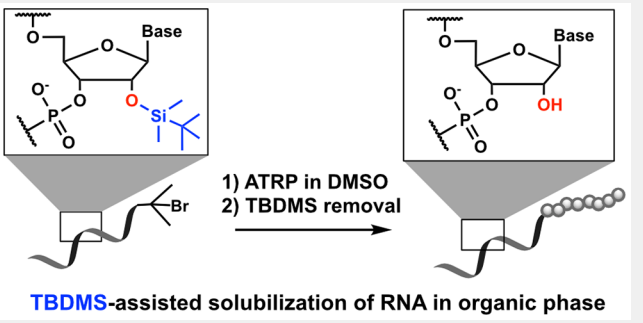

KEYWORDS: *ATRP, RNA, RNA-amphiphiles, nucleic acid block copolymer, RNA−polymer conjugate, TBDMS, SBiB, phosphoramidite, solid-phase RNA synthesis*

INTRODUCTION

As biologically active and programmable biopolymers, nucleic acids have been widely used as building blocks for multifunctional biomaterials.[1,2] The conjugation of nucleic acids with hydrophobic polymers provides a fascinating approach to developing novel biomaterials with the synergistically combined properties of nucleic acids and synthetic polymers.[3] Due to the solubility differences between the two distinct blocks, the amphiphilic nucleic acid bioconjugates show interesting self-assembly behavior in aqueous buffers forming micelles,[4] vesicles,[5] nanosheets,[6] and wormlike structures.[7]

The synthesis of amphiphilic nucleic acid conjugates has mostly been performed on the solid phase. The "blocking onto" approach (i.e., coupling of hydrophobic polymers with clickable functional groups (e.g., carboxylic acid, phosphoramidite, azide, norbornene, etc.) onto nucleic acids with complementary coupling handles) is the most commonly used synthetic method.[8−12] The "blocking from" approach (i.e., incorporation of a polymerization initiating moiety and subsequent polymerization of hydrophobic monomers from the nucleic acid on the solid support) has been reported.[13] Due to the heterogeneous nature of the reaction, coupling yields are often lower than in the solution phase. Therefore, several strategies for the coupling of presynthesized polymers onto nucleic acids in organic solvents have been reported through diverse coupling methods[14,15] or the use of cationic surfactants[16] to improve the coupling yield and the solubility of nucleic acids in organic solvents. Nonetheless, the steric hindrance during the coupling reaction between two macromolecules necessitates rigorous purification of the final products.[3] The homogeneous blocking from approach could be a powerful alternative for block copolymerization of hydrophobic polymers from hydrophilic nucleic acids with significantly reduced steric hindrance.[17,18] However, techniques enabling the solubilization of nucleic acid initiators in organic solvents and polymerization from the nucleic acid initiators in the organic solvent have not yet been developed.

Ribonucleic acid (RNA) is a particularly interesting type of nucleic acid due to its unique ability to regulate and catalyze a variety of cellular processes in addition to carrying genetic information.[19] However, studies on the RNA−polymer conjugates have remained in the early stage compared to their deoxygenated analogue (i.e., DNA, deoxyribonucleic acid).[20,21] One of the critical reasons for these phenomena could be the intrinsic instability of RNA: 2′-Hydroxyl (2′-OH)

Received: March 30, 2023
Revised: May 10, 2023
Accepted: May 12, 2023
Published: May 31, 2023

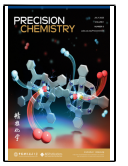

https://doi.org/10.1021/prechem.3c00042
Precis. Chem. 2023, 1, 326−331

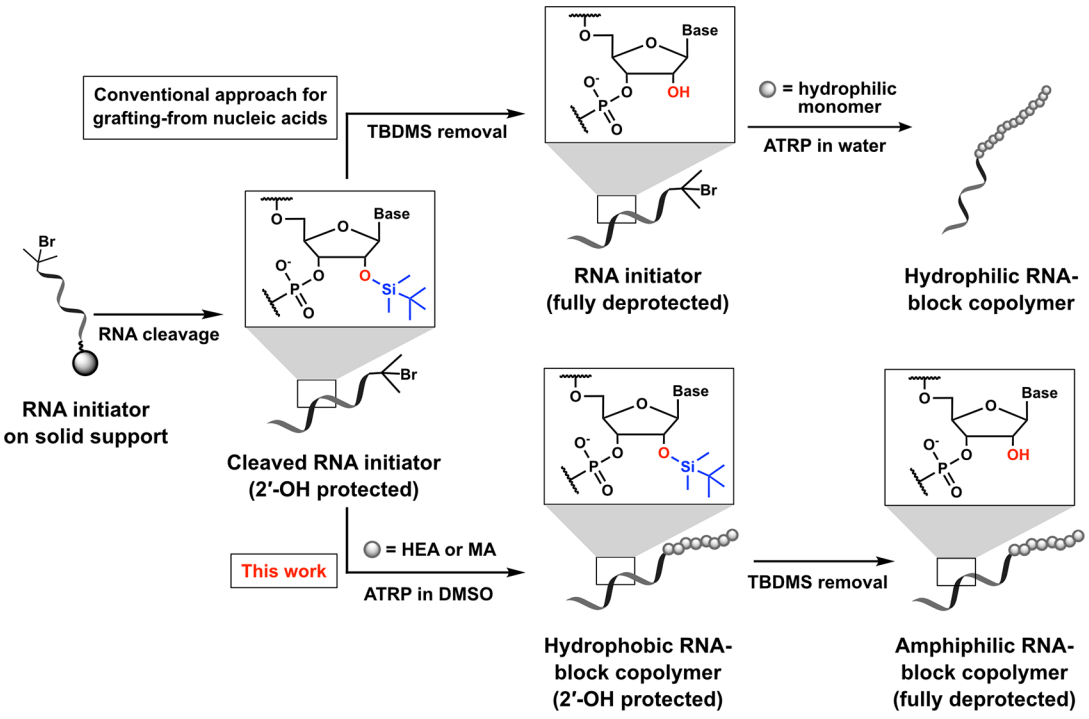

Figure 1. Block copolymerization from TBDMS-on RNA macroinitiator in DMSO. Scheme of polymerization from (top) deprotected RNA macroinitiator in an aqueous buffer and (bottom) TBDMS-on RNA macroinitiator in DMSO, respectively. TBDMS = *t*-butyldimethylsilyl group.

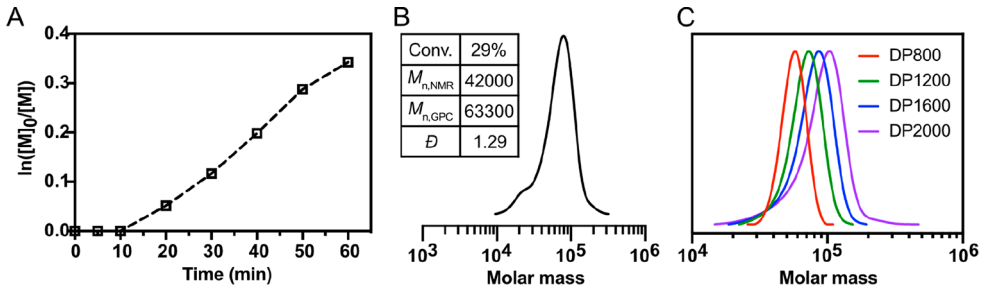

Figure 2. Block copolymerization of HEA from RNA macroinitiator with TBDMS ($U20_{on}$−SBiB) in DMSO. (A) The kinetic plot of the polymerization of HEA from $U20_{on}$−SBiB in DMSO. Reaction conditions: [HEA]/[$U20_{on}$−SBiB]/[$CuBr_2$]/[Me_6TREN]/[EYH_2] = 1000/1/0.5/3/0.002, [HEA] = 1600 mM, in DMSO for 60 min under green light irradiation (520 nm, 7.6 mW/cm^2). (B) DMF GPC trace (PMMA as the standard) of $U20_{on}$−pHEA hybrids with TBDMS on RNA after 60 min of polymerization in DMSO. (C) The molecular weight control experiment using HEA as a model monomer and the RNA macroinitiator with TBDMS ($U20_{on}$−SBiB). The degree of polymerization of the resulting pHEA was controlled by changing the $U20_{on}$−SBiB concentration as shown in Table S1. Reaction conditions: [HEA]/[$U20_{on}$−SBiB]/[$CuBr_2$]/[Me_6TREN]/[EYH_2] = 1000/0.5−1.25/0.5/3/0.002, [HEA] = 1600 mM, in DMSO for 30 min under green light irradiation (520 nm, 7.6 mW/cm^2).

groups in RNA monomer units (i.e., ribonucleotides) can attack the vicinal phosphodiester bond, resulting in cleavage.

Herein, we report a strategy to circumvent the limitations of previously reported methods for the synthesis of RNA−polymer amphiphiles: poor solubility of RNA in organic solvents and poor chemical stability of RNA caused by 2′-OH groups. We were inspired by phosphoramidite chemistry which has been a gold standard for oligonucleotide synthesis.[22] In the conventional approach, nucleic acid containing a polymerization initiation residue is synthesized in the solid phase using an oligonucleotide synthesizer followed by cleavage and deprotection of nucleobases. Subsequently, *t*-butyldimethylsilyl (TBDMS) groups on the 2′-hydroxyl groups in RNA are removed by treatment with triethylamine trihydrofluoride (TEA·3HF), yielding the fully deprotected RNA macroinitiator that can later be used for the polymerization of hydrophilic monomers in aqueous buffer.[13,23] We focused here on the RNA macroinitiator that is cleaved from the solid support while leaving the protecting groups (TBDMS) on the 2′-OH groups. We envisioned that the TBDMS groups would improve the solubility of the RNA macroinitiator in an organic solvent (i.e., DMSO)[24] and enable the polymerization of hydrophobic monomers from the RNA macroinitiator while inhibiting 2′-OH group-mediated cleavage (Figure 1).

RESULTS AND DISCUSSION

To synthesize the RNA macroinitiator using an oligonucleotide synthesizer, the ATRP initiator-functionalized phosphoramidite was prepared using serinol as the starting material (Figure S1). Precise and high-yield phosphoramidite chemistry provided a robust and automated approach for incorporating ATRP initiator into nucleic acids.[13,25] The structure of the final

https://doi.org/10.1021/prechem.3c00042
Precis. Chem. 2023, 1, 326−331

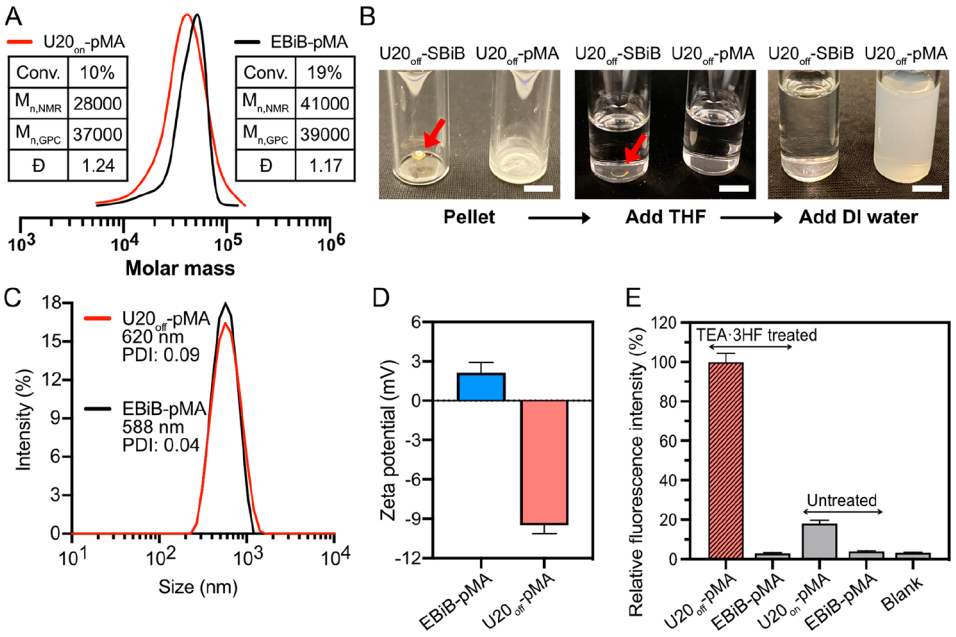

Figure 3. Block copolymerization of MA from RNA macroinitiator with TBDMS ($U20_{on}$–SBiB) in DMSO. (A) DMF GPC traces of pMA initiated by $U20_{on}$–SBiB ($U20_{on}$–pMA) and EBiB (EBiB–pMA) in DMSO. Reaction conditions: [MA]/[Initiator]/[$CuBr_2$]/[Me_6TREN]/[EYH_2] = 2500/1/1.25/7.5/0.004, [M] = 5500 mM, in DMSO under green light irradiation (520 nm, 7.6 mW/cm^2) for 30 min. The GPC was calibrated to PMMA (DMF as an eluent). (B) A comparison of the solubility of deprotected RNA macroinitiator ($U20_{off}$–SBiB) and $U20_{off}$–pMA conjugate without TBDMS in THF and 1:1 THF:water mixture, respectively. 500 μL of THF and 500 μL of water were sequentially added to 1.5 mg of each substrate. Scale bars, 5 mm. (C) DLS trace of $U20_{off}$–pMA and EBiB–pMA dialyzed in water. (D) Zeta potential of $U20_{off}$–pMA and EBiB–pMA in water. (E) Confirmation of removal of TBDMS groups in the $U20_{on}$–pMA hybrids after polymerization. 0.5 mg of each sample was stained with SYBR Gold dye. The fluorescence intensity of SYBR Gold was recorded by a microplate reader (ex: 493 nm; em: 537 nm).

product, serinol-based α-bromoisobutyryl (SBiB) phosphoramidite, was confirmed by ^{1}H NMR (Figures S2–S4), ^{13}C NMR, and ^{31}P NMR (Figure S5) spectroscopy.

As a model RNA macroinitiator for polymerization in an organic solvent (i.e., DMSO), oligo uridine with one SBiB residue at the 5′ terminus (U20–SBiB) was synthesized using a solid-phase oligonucleotide synthesizer using standard RNA synthesis conditions. After the synthesis, the RNA macroinitiator was cleaved from the solid support, yielding 20-mer oligo uridine with terminal SBiB and protecting groups (i.e., TBDMS) on the 2′-hydroxyl groups ($U20_{on}$–SBiB). The resulting $U20_{on}$–SBiB was lyophilized, dissolved in anhydrous DMSO, and stored at −20 °C until use. The $U20_{on}$–SBiB was characterized by MALDI-TOF (Figure S6).

All the polymerization reactions in this study were performed using a recently developed photoinduced ATRP technique that is mediated by eosin Y (EYH_2) and copper catalyst under green light irradiation (Figure S7).[26,27] Due to its excellent oxygen tolerance and well-controlled polymerization behavior under physiological conditions, this technique allows polymerization using biomolecule initiators at low volume (i.e., 250 μL) without the deoxygenation processes.[28] We have used this mild ATRP method successfully with DNA and also with RNA in the conventional approach to polymer hybrids. Here, our initial study started by investigating the polymerization kinetics of block copolymerization from RNA in DMSO using hydroxyethyl acrylate (HEA) as the model monomer at the target degree of polymerization (DP_T) of 1000. As shown in Figure 2A, after a short induction period of 10 min, monomer conversion reached 29% after 60 min of green light irradiation (Figure S8). The resulting block copolymer was analyzed by gel permeation chromatography (using DMF as eluent) as demonstrated in Figure 2B. The RNA–polymer hybrid with a relatively narrow molecular weight distribution ($Đ$) of 1.29 was formed. However, a discrepancy between the theoretical molecular weight calculated from monomer conversion ($M_{n,NMR}$) and the apparent molecular weight obtained from GPC ($M_{n,GPC}$) was observed. This is likely due to some termination reactions as evidenced by the low molar mass shoulder on the GPC trace (Figure 2B). Of note, the low concentration of initiator relative to monomer can lead to a more pronounced radical termination and less-efficient initiation which often results in lower monomer conversion and higher dispersity. To limit the effect of these side reactions, it is desired to use a higher monomer concentration (i.e., to use a monomer as a diluent and to favor propagation over termination), stop the polymerization at low monomer conversion, and remove unreacted monomer by dialysis.

Then, we explored the possibility of controlling the molecular weight of poly(2-hydroxyethyl acrylate) (pHEA) grown from $U20_{on}$–SBiB in DMSO (Figure 2C). Notably, the ATRP was performed for 30 min to minimize the termination reaction observed in Figure 2B. Interestingly, the GPC traces shown in Figure 2C indicate successful molecular weight control of the pHEA chain grown from RNA. However, a small deviation between theoretical molecular weight ($M_{n,NMR}$) and $M_{n,GPC}$ in addition to tailings toward low molecular weights in the GPC traces were noticed (Table S1). This could be due to the relatively low initiation efficiency of α-bromoalkyl amide ATRP initiators in organic solvents compared to ester-based initiators.[29−31] Nonetheless, low dispersities of the resulting RNA–pHEA conjugates ($U20_{on}$–pHEA) in the range of

https://doi.org/10.1021/prechem.3c00042
Precis. Chem. 2023, 1, 326−331

1.04−1.18 confirmed the synthesis of the homogeneous RNA amphiphiles (Table S1).

After the successful polymerization of HEA, we tested the polymerization of a less polar monomer to examine the versatility of our polymerization methodology in DMSO. Methyl acrylate (MA) was chosen as a model monomer due to the poor solubility and precipitation of the resulting polymer in the presence of water. Using the identical RNA macroinitiator used for the polymerization of HEA ($U20_{on}$−SBiB), we performed polymerization of MA in DMSO at the monomer concentration of 5.5 M. We targeted polymerization at DP_T = 2500 (Figure 3A). A slightly lower conversion of MA (10%) was observed after 30 min of polymerization compared to the result of HEA (20−27%) due to the higher target degree of polymerization. Dispersity of 1.24 and nearly symmetrical GPC traces confirmed the successful polymerization of MA from RNA in DMSO. We also performed polymerization using a conventional ATRP initiator (i.e., EBiB, ethyl α-bromoisobutyrate) as a control. A higher conversion of monomer and pMA with lower $Đ$ was formed when initiated by EBiB (EBiB−pMA) as compared to pMA formed from RNA macroinitiator ($U20_{on}$−pMA), as shown in Figure 3A. Similar to the result in Figure 2, this is presumably due to the lower activity and initiation efficiency of the amido-based ATRP initiator (SBiB residue in $U20_{on}$−SBiB) compared to ester-based ATRP initiators (EBiB). The trend was also noticed for polymerization results targeting higher DP_T = 5500 (Figure S9). Polymerization of MA in DMSO using the similar, but deprotected RNA macroinitiator without TBDMS ($U20_{off}$−SBiB) was also performed (Figure S10). However, due to insufficient solubility of the fully deprotected RNA in DMSO, the RNA remained as a pellet and no polymerization was observed.

Next, TEA·3HF was added to the $U20_{on}$−pMA to remove TBDMS groups in the conjugate. After incubation for 2.5 h at 65 °C, the resulting RNA−pMA block copolymer conjugate without TBDMS ($U20_{off}$−pMA) was collected by precipitation in water. As shown in Figure 3B, the attached pMA residue in RNA assisted the solubilization of the RNA in tetrahydrofuran (THF), and the $U20_{off}$−pMA conjugate was completely dissolved in THF. In contrast, $U20_{off}$−SBiB, the deprotected RNA macroinitiator without a hydrophobic motif (i.e., pMA), remained as a pellet after the addition of THF. The addition of water to the $U20_{off}$−pMA resulted in the precipitation of the conjugate due to the poor solubility of pMA in water (Figure 3B and Figure S11).

We further characterized the pMA grown from the RNA macroinitiator (i.e., $U20_{off}$−pMA) and the pMA initiated from EBiB (i.e., EBiB−pMA) by dynamic light scattering (DLS) and zeta potential measurements. Similar size and polydispersity index (PDI) of $U20_{off}$−pMA and EBiB−pMA were recorded (Figure 3C), likely due to the similar molecular weight ($M_{n,GPC}$) of the two conjugates (Figure 3A). Interestingly, a negative zeta potential value of $U20_{off}$−pMA was observed while EBiB−pMA showed a slightly positive value. This indicates that the RNA moiety in the $U20_{off}$−pMA conjugate is located outside in the aqueous buffer due to the superior solubility of deprotected RNA, as compared to synthetic hydrophobic polymers, consistent with previous results.[13,32]

We then removed TBDMS from the RNA in the RNA−pMA amphiphile. To confirm the deprotection of hydroxyl groups in the RNA, we stained the $U20_{off}$−pMA conjugates with SYBR Gold, the RNA-staining fluorogenic dye. The presence of TBDMS on RNA should inhibit the intercalation of SYBR Gold dyes within the RNA strands, preventing SYBR Gold dye from emitting strong fluorescence.[33,34] As expected, strong fluorescence of SYBR Gold was only observed when SYBR Gold was added to the RNA−pMA conjugate after TEA·3HF treatment and TBDMS removal (i.e., $U20_{off}$−pMA). In contrast, the RNA−pMA conjugate with TBDMS ($U20_{on}$−pMA) or control groups (EBiB−pMA with or without TEA·3HF treatment) did not show strong fluorescence of SYBR Gold. In addition, we confirmed that the TEA·3HF treatment did not cause significant hydrolysis of ester groups in the pMA residue using GPC (Figure S12) and ^{1}H NMR (Figure S13). The results demonstrate that TBDMS in the RNA−polymer conjugate can be removed after polymerization, yielding deprotected RNA−polymer amphiphiles.

To confirm the generality and mildness of the conditions for a mixed sequence RNA in which the nucleobases are protected, and the integrity of the RNA after polymerization and deprotection, we synthesized a 15-mer RNA strand with a photocleavable linker between RNA and SBiB residue with TBDMS groups left on ($Rpc15_{on}$−SBiB; Figure S14). After polymerization of MA from $Rpc15_{on}$−SBiB, the RNA was fully deprotected with TEA·3HF treatment and released from the pMA chain by UV irradiation, and the RNA was characterized by MALDI-TOF analysis (Figure S14C). We observed a good agreement between the molecular weight and its predicted value, confirming the stability of the TBDMS-protected RNA during the polymerization process.

CONCLUSIONS

In conclusion, we have demonstrated the photoinduced ATRP of hydrophobic monomers using an organic-phase-soluble RNA macroinitiator. The solid-phase incorporation of ATRP initiator (i.e., SBiB) into RNA and the subsequent cleavage and deprotection of nucleobases facilitated the preparation of a RNA macroinitiator with TBDMS groups on 2′-hydroxyl groups which assisted solubilization of RNA in DMSO. The TBDMS-protected RNA macroinitiator was successfully utilized for the polymerization of the model monomers, HEA and hydrophobic MA, in DMSO. Our results indicate that RNA−polymer amphiphiles can be fabricated by the "blocking-from" approach in DMSO, which has not yet been reported. We envision that this methodology can be further applied to the preparation of a variety of RNA−polymer conjugates that exhibit unique applications, including self-assembly and drug delivery.

ASSOCIATED CONTENT

Supporting Information

The Supporting Information is available free of charge at https://pubs.acs.org/doi/10.1021/prechem.3c00042.

Additional experimental details and information including ^{1}H, ^{13}C, and ^{31}P NMR, digital camera images of the polymerization setup, additional GPC results, mass spectra, and a table of the summary of reaction conditions and results (PDF)

AUTHOR INFORMATION

Corresponding Authors

Subha R. Das − *Department of Chemistry, Carnegie Mellon University, Pittsburgh, Pennsylvania 15213, United States;*

https://doi.org/10.1021/prechem.3c00042
Precis. Chem. 2023, 1, 326−331

Center for Nucleic Acids Science & Technology, Carnegie Mellon University, Pittsburgh, Pennsylvania 15213, United States; orcid.org/0000-0002-5353-0422; Email: srdas@andrew.cmu.edu

Krzysztof Matyjaszewski − *Department of Chemistry, Carnegie Mellon University, Pittsburgh, Pennsylvania 15213, United States;* orcid.org/0000-0003-1960-3402; Email: km3b@andrew.cmu.edu

Authors

Jaepil Jeong − *Department of Chemistry, Carnegie Mellon University, Pittsburgh, Pennsylvania 15213, United States; Center for Nucleic Acids Science & Technology, Carnegie Mellon University, Pittsburgh, Pennsylvania 15213, United States*

Grzegorz Szczepaniak − *Department of Chemistry, Carnegie Mellon University, Pittsburgh, Pennsylvania 15213, United States; University of Warsaw, Faculty of Chemistry, 02-093 Warsaw, Poland;* orcid.org/0000-0002-0355-9542

Complete contact information is available at: https://pubs.acs.org/10.1021/prechem.3c00042

Notes

The authors declare no competing financial interest.

■ ACKNOWLEDGMENTS

We gratefully acknowledge financial support from NSF DMR 2202747 and DTRA grant HDTRA1-20-1-0014. G.S. gratefully acknowledges the Polish National Agency for Academic Exchange (BPN/PPO/2022/1/00027) for financial support.

■ REFERENCES

(1) Messina, M. S.; Messina, K. M. M.; Bhattacharya, A.; Montgomery, H. R.; Maynard, H. D. Preparation of biomolecule-polymer conjugates by grafting-from using ATRP, RAFT, or ROMP. *Prog. Polym. Sci.* **2020**, *100*, 101186.

(2) Li, J.; Green, A. A.; Yan, H.; Fan, C. Engineering nucleic acid structures for programmable molecular circuitry and intracellular biocomputation. *Nat. Chem.* **2017**, *9* (11), 1056−1067.

(3) Lu, H.; Cai, J.; Zhang, K. Synthetic approaches for copolymers containing nucleic acids and analogues: challenges and opportunities. *Polym. Chem.* **2021**, *12* (15), 2193−2204.

(4) Chien, M. P.; Rush, A. M.; Thompson, M. P.; Gianneschi, N. C. Programmable shape-shifting micelles. *Angew. Chem., Int. Ed.* **2010**, *49* (30), 5076−5080.

(5) Rodríguez-Pulido, A.; Kondrachuk, A. I.; Prusty, D. K.; Gao, J.; Loi, M. A.; Herrmann, A. Light-triggered sequence-specific cargo release from DNA block copolymer-lipid vesicles. *Angew. Chem., Int. Ed.* **2013**, *52* (3), 1008−1012.

(6) Kim, C.-J.; Park, J.-e.; Hu, X.; Albert, S. K.; Park, S.-J. Peptide-driven shape control of low-dimensional DNA nanostructures. *ACS Nano* **2020**, *14* (2), 2276−2284.

(7) Lückerath, T.; Koynov, K.; Loescher, S.; Whitfield, C. J.; Nuhn, L.; Walther, A.; Barner-Kowollik, C.; Ng, D. Y.; Weil, T. DNA-Polymer Nanostructures by RAFT Polymerization and Polymerization-Induced Self-Assembly. *Angew. Chem., Int. Ed.* **2020**, *59* (36), 15474−15479.

(8) Alemdaroglu, F. E.; Alemdaroglu, N. C.; Langguth, P.; Herrmann, A. DNA block copolymer micelles-a combinatorial tool for cancer nanotechnology. *Adv. Mater.* **2008**, *20* (5), 899−902.

(9) Rafique, M. G.; Remington, J. M.; Clark, F.; Bai, H.; Toader, V.; Perepichka, D. F.; Li, J.; Sleiman, H. F. Two-Dimensional Supramolecular Polymerization of DNA Amphiphiles is Driven by Sequence-Dependent DNA-Chromophore Interactions. *Angew. Chem. Int. Ed.* **2023**, No. e202217814.

(10) Trinh, T.; Liao, C.; Toader, V.; Barłóg, M.; Bazzi, H. S.; Li, J.; Sleiman, H. F. DNA-imprinted polymer nanoparticles with monodispersity and prescribed DNA-strand patterns. *Nat. Chem.* **2018**, *10* (2), 184−192.

(11) Jiang, T.; Qiao, Y.; Ruan, W.; Zhang, D.; Yang, Q.; Wang, G.; Chen, Q.; Zhu, F.; Yin, J.; Zou, Y.; et al. Cation-Free siRNA Micelles as Effective Drug Delivery Platform and Potent RNAi Nanomedicines for Glioblastoma Therapy. *Adv. Mater.* **2021**, *33* (45), 2104779.

(12) Roloff, A.; Nelles, D. A.; Thompson, M. P.; Yeo, G. W.; Gianneschi, N. C. Self-transfecting micellar RNA: modulating nanoparticle cell interactions via high density display of small molecule ligands on micelle coronas. *Bioconjugate Chem.* **2018**, *29* (1), 126−135.

(13) Averick, S. E.; Dey, S. K.; Grahacharya, D.; Matyjaszewski, K.; Das, S. R. Solid-Phase Incorporation of an ATRP Initiator for Polymer-DNA Biohybrids. *Angew. Chem., Int. Ed.* **2014**, *53* (10), 2739−2744.

(14) Wilks, T. R.; O'Reilly, R. K. Efficient DNA-Polymer coupling in organic solvents: a survey of amide coupling, thiol-ene and tetrazine-norbornene chemistries applied to conjugation of poly (N-Isopropylacrylamide). *Sci. Rep.* **2016**, *6* (1), 1−11.

(15) Wilks, T. R.; Bath, J.; de Vries, J. W.; Raymond, J. E.; Herrmann, A.; Turberfield, A. J.; O'Reilly, R. K. Giant surfactants" created by the fast and efficient functionalization of a DNA tetrahedron with a temperature-responsive polymer. *ACS Nano* **2013**, *7* (10), 8561−8572.

(16) Liu, K.; Zheng, L.; Liu, Q.; de Vries, J. W.; Gerasimov, J. Y.; Herrmann, A. Nucleic acid chemistry in the organic phase: from functionalized oligonucleotides to DNA side chain polymers. *J. Am. Chem. Soc.* **2014**, *136* (40), 14255−14262.

(17) Baker, S. L.; Kaupbayeva, B.; Lathwal, S.; Das, S. R.; Russell, A. J.; Matyjaszewski, K. Atom Transfer Radical Polymerization for Biorelated Hybrid Materials. *Biomacromolecules* **2019**, *20* (12), 4272−4298.

(18) Matyjaszewski, K. Advanced Materials by Atom Transfer Radical Polymerization. *Adv. Mater.* **2018**, *30* (23), 1706441.

(19) Dykstra, P. B.; Kaplan, M.; Smolke, C. D. Engineering synthetic RNA devices for cell control. *Nat. Rev. Genet.* **2022**, *23* (4), 215−228.

(20) Kim, H.; Park, Y.; Kim, J.; Jeong, J.; Han, S.; Lee, J. S.; Lee, J. B. Nucleic acid engineering: RNA following the trail of DNA. *ACS Comb. Sci.* **2016**, *18* (2), 87−99.

(21) Whitfield, C. J.; Zhang, M.; Winterwerber, P.; Wu, Y.; Ng, D. Y.; Weil, T. Functional DNA-polymer conjugates. *Chem. Rev.* **2021**, *121* (18), 11030−11084.

(22) Beaucage, S.; Caruthers, M. Deoxynucleoside phosphoramidites—a new class of key intermediates for deoxypolynucleotide synthesis. *Tetrahedron Lett.* **1981**, *22* (20), 1859−1862.

(23) Lin, E.-W.; Maynard, H. D. Grafting from small interfering ribonucleic acid (siRNA) as an alternative synthesis route to siRNA-polymer conjugates. *Macromolecules* **2015**, *48* (16), 5640−5647.

(24) Tan, X.; Lu, H.; Sun, Y.; Chen, X.; Wang, D.; Jia, F.; Zhang, K. Expanding the materials space of DNA via organic-phase ring-opening metathesis polymerization. *Chem.* **2019**, *5* (6), 1584−1596.

(25) Tokura, Y.; Jiang, Y.; Welle, A.; Stenzel, M. H.; Krzemien, K. M.; Michaelis, J.; Berger, R.; Barner-Kowollik, C.; Wu, Y.; Weil, T. Bottom-Up Fabrication of Nanopatterned Polymers on DNA Origami by In Situ Atom-Transfer Radical Polymerization. *Angew. Chem.* **2016**, *128* (19), 5786−5791.

(26) Szczepaniak, G.; Jeong, J.; Kapil, K.; Dadashi-Silab, S.; Yerneni, S. S.; Ratajczyk, P.; Lathwal, S.; Schild, D. J.; Das, S. R.; Matyjaszewski, K. Open-air green-light-driven ATRP enabled by dual photoredox/copper catalysis. *Chem. Sci.* **2022**, *13* (39), 11540−11550.

(27) Kapil, K.; Szczepaniak, G.; Martinez, M. R.; Murata, H.; Jazani, A. M.; Jeong, J.; Das, S. R.; Matyjaszewski, K. Visible-Light-Mediated Controlled Radical Branching Polymerization in Water. *Angew. Chem., Int. Ed.* **2023**, *62*, No. e202217658.

(28) Szczepaniak, G.; Fu, L.; Jafari, H.; Kapil, K.; Matyjaszewski, K. Making ATRP More Practical: Oxygen Tolerance. *Acc. Chem. Res.* **2021**, *54* (7), 1779−1790.
(29) Tang, W.; Matyjaszewski, K. Effects of Initiator Structure on Activation Rate Constants in ATRP. *Macromolecules (Washington, DC, United States)* **2007**, *40* (6), 1858−1863.
(30) Ribelli, T. G.; Lorandi, F.; Fantin, M.; Matyjaszewski, K. Atom Transfer Radical Polymerization: Billion Times More Active Catalysts and New Initiation Systems. *Macromol. Rapid Commun.* **2019**, *40* (1), 1800616.
(31) Matyjaszewski, K. Atom Transfer Radical Polymerization (ATRP): Current Status and Future Perspectives. *Macromolecules (Washington, DC, U. S.)* **2012**, *45* (10), 4015−4039.
(32) Kim, C.-J.; Hu, X.; Park, S.-J. Multimodal shape transformation of dual-responsive DNA block copolymers. *J. Am. Chem. Soc.* **2016**, *138* (45), 14941−14947.
(33) Cosa, G.; Focsaneanu, K. S.; McLean, J.; McNamee, J.; Scaiano, J. Photophysical Properties of Fluorescent DNA-dyes Bound to Single-and Double-stranded DNA in Aqueous Buffered Solution¶. *Photochem. Photobiol.* **2001**, *73* (6), 585−599.
(34) Biebricher, A. S.; Heller, I.; Roijmans, R. F.; Hoekstra, T. P.; Peterman, E. J.; Wuite, G. J. The impact of DNA intercalators on DNA and DNA-processing enzymes elucidated through force-dependent binding kinetics. *Nat. Commun.* **2015**, *6* (1), 7304.

https://doi.org/10.1021/prechem.3c00042
Precis. Chem. 2023, 1, 326−331